

Broadband thermal light with Bose-Einstein photon statistics from warm atomic vapor

J. Mika, L. Podhora, L. Lachman, P. Obšil, J. Hloušek, M. Ježek, R. Filip, and L. Slodička*
Department of Optics, Palacký University, 17. listopadu 1192/12, 771 46 Olomouc, Czech Republic

We present the experimental observation of light with ideal thermal statistics generated in a warm atomic vapor. Statistical properties of the generated light field are tested both by the direct measurement of second-order correlation function and by the detailed analysis of photon number distribution, which certifies the quality of the Bose-Einstein statistics generated by natural physical mechanism. We further demonstrate the extension of spectral bandwidth of the generated light to hundreds of MHz domain while keeping the ideal thermal statistics, which suggests a direct applicability of the presented source in a broad range of applications including optical metrology, quantum imaging, tests of robustness of quantum communication protocols, or quantum thermodynamics.

I. INTRODUCTION

Generation of light statistics has been of paramount importance for understanding various physical phenomena in classical and quantum domain since the presentation of pioneering experiments by R. Hanbury Brown and R. Q. Twiss in 1956 [1, 2]. The advent of lasers has triggered a prompt application of methods for estimation of light statistics on studies in broad range of research directions ranging from atomic spectroscopy to optical imaging and metrology, reaching far beyond the areas of pure optical physics and astronomy. The strong promise of application of well controlled quantum systems in quantum communication networks in last two decades led a large part of quantum optics community to focus on the development and characterization of the nonclassical light sources [3, 4]. Together with the further development of field of quantum statistical optics [5], the generation and control of nonclassical light states stimulated enormous effort on technical improvements in control of various degrees of freedom of light fields at single photon level and their efficient and fast detection, a crucial requirements for direct observability of intrinsically quantum properties [6, 7]. These technical developments have been extensively applied on witnessing of subtle characteristics of nonclassical states of light in experiments mostly represented by observation of good approximations of single-photon states [3, 4]. Ideal single-photon states have vanishing variance of the photon number distribution accompanied with characteristic strong antibunching in the measured degree of second-order coherence.

However, a large number of research directions in optical physics has recently rediscovered the strong application potential of light fields with exactly opposite statistical properties, that is, strong photon bunching and super-Poissonian fluctuations of the photon number. From an infinite set of these states, the ideal thermal state corresponding to idealized population of the single light field mode by thermal excitations is of very significant importance. Thermal state has a maximum entropy for the given constant average energy and so it uniquely

determines the Bose-Einstein statistics of any mode of thermal radiation. As such, this statistics naturally appears at thermal equilibrium. Ideal thermal radiation can be directly applied in diagnostics of quantum states and processes [8–10], enhancement of nonlinear effects and metrology [11–13], quantum imaging [14–16], generation of nonclassicality [17], or pioneering tests of quantum thermodynamics [18] and quantum key distribution [19].

Although thermal light field is fully described by the classical Maxwell theory of light waves, their successful experimental generation and detection shares number of difficulties typically associated with demonstrations of fragile quantum properties of light. These include strict requirements on the observed field modeness and photon detection bandwidth, particularly when aiming for direct observation of thermal statistics of photons from a source at thermal equilibrium. These difficulties have been recognized by number of experimental teams and led to a broad employment of pseudo-thermal light sources typically based on the scattering of a laser beam from rotating ground-glass disc [20–22]. Although such approach can emulate thermal light field with very high fidelity, it is technically limited in the achievable spectral bandwidths due to practically achievable disk rotation speeds, average grain spatial size and focal spot of the scattered laser beam to a few MHz range [23]. In addition, such generation lacks some fundamental properties of a true thermal light [24]. However, it is the actual spectral bandwidth which represents a crucial parameter for potential improvement of waste majority of applications of thermal light [8–16]. On one side it directly relates to the efficiency of various processes and on the other, it allows for increasing their repetition rates.

The first realization of a thermal light source with directly observable ideal bunching, besides the pseudo-thermal light sources utilizing the bare intensity modulation of coherent light beam, was reported in 2010 in [25]. There, the generation of light was based on the excitation of laser-cooled atomic cloud and the provided analysis of the second-order coherence of contributing scattering processes quantitatively supported the observed bunching. Besides the relatively high technical demands of the presented setup given by the necessity of laser cooling and isolation of atoms from the thermal environment,

* slodicka@optics.upol.cz

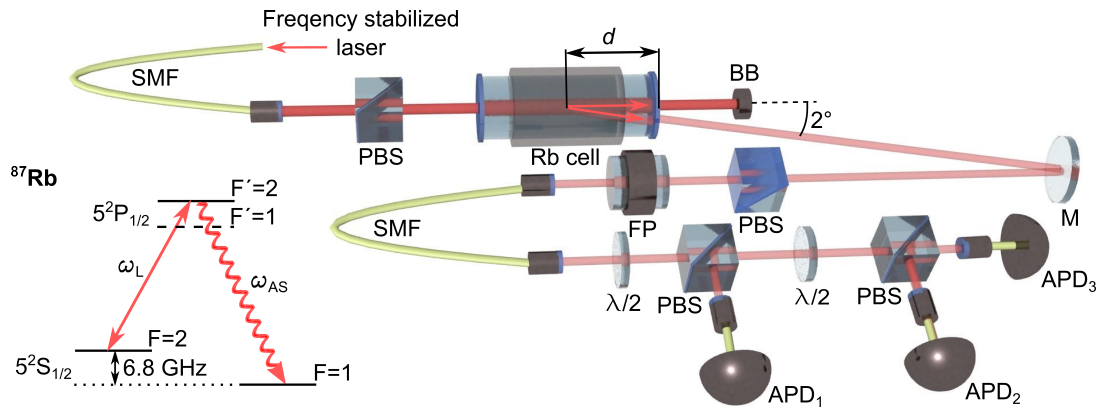


FIG. 1. The schematic setup of the presented experiment and employed ^{87}Rb energy level scheme. The polarization and spatial mode of the laser beam emitted from the frequency stabilized laser diode are defined by the input single-mode optical fiber (SMF) and polarization beam splitter (PBS). The laser beam excites an ensemble of warm ^{87}Rb atoms and the scattered light is observed under small angle of approximately 2° . The mode of the detected light field is defined precisely using the combination of a Glan-Thompson polarizer (G-T), Fabry-Pérot resonator (FP) and single mode fiber. The photon statistics of the field is analyzed using an array of single-photon avalanche detectors (APD_{1-3}) with balanced detection efficiencies. The balancing is achieved by tuning the $\lambda/2$ polarization half-wave plates in front of each PBS. BB marks beam block, M is the optical mirror and d corresponds to spatial distance between the observation region and atomic cell output window.

such source imposes strong limits on the easily achievable spectral widths of the emitted radiation due to narrow emission spectra of the bare atomic transitions. A number of experimental teams have recently tried to realize a thermal light source with large spectral bandwidth either as a principal resource or as a side result of attempts to engineer a nonlinear interaction with a high degree of mode purity [12, 26–32]. Out of these, the sources utilizing the process of amplified spontaneous emission [12, 30–32] seem to offer technically feasible spectral bandwidth in a few nanometer regime. However, similarly to several characterizations of light statistics coming from black-body light sources [33, 34], the extreme spectral width practically hinders a direct confirmation of ideal thermal statistics with currently available single-photon detectors. Several promising techniques have been developed to circumvent the limited detection bandwidths, including the schemes based on the two-photon absorption [30], or nonlinear sum frequency generation [11, 35, 36]. However, even these remarkable technological advancements did not lead to direct unambiguous observation of ideal thermal light with large spectral bandwidth.

Here, we report on a direct measurement of ideal Bose-Einstein photon statistics on light generated by the excitation of warm atomic vapor and demonstrate its traceable extension to observable spectral bandwidths at the order of Doppler-broadened atomic transition lines. The observability of the ideal photon bunching is achieved by the satisfaction of two fundamental experimental requirements, high single modeness of the detected light and sufficiently narrow spectral bandwidth relative to the timing jitter of the employed single photon detectors. They result in directly measurable Bose-Einstein statistics of generated light, which allows the evaluation of entropy for given mean photon number. We provide an

experimental guideline for achieving the large bandwidth ideal thermal light and outline the limits on the achievable spectral bandwidths and generated photon rates of thermal source based on the presented experimental platform.

II. GENERATION OF IDEAL THERMAL LIGHT

Our experimental demonstration is based on phenomenologically simple excitation of warm ^{87}Rb vapor with a laser beam in a single-pass configuration and observation of the scattered light field after precise spatial, polarization and spectral filtering, with the spectral filtering bandwidth surpassing the limit imposed by the finite timing jitters of the employed single photon detectors and the energy splitting of the excited atomic states hyperfine manifolds. The thermal statistics of individual single fluorescence light modes in our scheme results from the effective partial trace over one mode of the two-mode squeezed vacuum state in the spontaneous FWM process [37, 38]. This way of generation theoretically guarantees a high quality of thermal statistics. The relevant energy level scheme is depicted in Fig. 1. A travelling-wave strong resonant excitation of warm ^{87}Rb atoms on D1-line $5S_{1/2}(F=2) \leftrightarrow 5P_{1/2}(F'=2)$ transition and frequency selection of the anti-Stokes field generated through Raman transition $5S_{1/2}(F=2) \rightarrow 5P_{1/2}(F'=2) \rightarrow 5S_{1/2}(F=1)$ results in observation of single mode of a two-mode state generated in spontaneous FWM between four light fields with frequencies $(\nu_L, \nu_S, \nu_{AS} \sim \nu_L - 6.8 \text{ GHz}, \nu_{AS} \sim \nu_L + 6.8 \text{ GHz})$, where ν_L is the excitation laser frequency and ν_S and ν_{AS} denote the frequencies of Stokes and anti-Stokes fields, respec-

tively. The frequency 6.8 GHz corresponds to the splitting of ^{87}Rb $5S_{1/2}$ ground state hyperfine manifold. We note that, compared to experiments aiming for observation of nonclassical two-photon correlations or two-mode squeezing [28, 38], the presented experiment on observation of thermal light statistics does not require spatial alignment and optimization of the FWM phase matching, as we intend to trace over the second generated field mode anyway. This effectively allows the exploitation of the spontaneous FWM process for generation of thermal light also in phase-matching configurations which would be otherwise very inconvenient for achieving strong two-mode correlations with long coherence times, provided that it allows us to efficiently suppress the excitation laser light in the observation mode.

The excitation laser beam with wavelength of 795 nm is derived from the frequency stabilized laser diode and its spatial mode is set by a single-mode optical fiber (SMF), see Fig. 1 for the simplified scheme of the experimental arrangement. The polarization of the output Gaussian beam is adjusted to horizontal with respect to the plane defined by the optical table. The laser excites a warm atomic ensemble enclosed in a cylindrical glass cell of 7.5 cm length and 2.5 cm diameter with antireflection coated windows and with the Gaussian beam radius at the cell position of $440 \pm 10 \mu\text{m}$. The cell is filled with isotopically pure ^{87}Rb and contains no buffer gas or atomic polarization preserving coatings. The polarization of atomic fluorescence scattered at an angle of 2° is filtered to linear polarization perpendicular to the polarization of the excitation beam to suppress the detection of the light coming from the residual laser reflections. The fluorescence further passes a Fabry-Pérot resonator with the measured free spectral range $\text{FSR} = 8854 \pm 6 \text{ MHz}$ and the transmission linewidth of $\Delta\nu = 67 \pm 7 \text{ MHz}$ (FWHM). The resonator transmission frequency can be precisely tuned on the scale of its FSR by controlling the temperature of its Zerodur glass spacer. The FSR has been chosen to be larger than the ^{87}Rb emission spectra which guarantees the selection of a single particular emission frequency mode and, at the same time, the sufficiently narrow transmission linewidth $\Delta\nu$ allows for the selection of at most single radiative transition in the ^{87}Rb D_1 -line manifold. The relatively small transmission bandwidth of the employed optical resonator is also crucial for the unambiguous direct detection of the ideal thermal state, as it narrows the emitted Doppler-broadened emission spectra to bandwidths within the limit imposed by finite detection jitters on the order of hundreds of ps of conventional single-photon avalanche detectors operating in the visible spectral range [3]. After passing the optical cavity, the atomic fluorescence is coupled to a single-mode fiber which guarantees the spatial purity of the detected field mode. The fluorescence is analyzed in a spatially multiplexed array of three single photon avalanche photodiodes (APDs, Excelitas Technologies, SPCM CD3432H), where the effective individual detection efficiencies have been adjusted to close to equal values using a simple

polarization-manipulation scheme comprising the polarization rotation by half-wave plates (HWP) and spatial separation on polarization beam splitters (PBS). The presented photon-detection configuration allows for evaluation of typical statistical characteristics of thermal light manifested in the shape and absolute values of the normalized second-order correlation function $g^{(2)}(\tau) = \langle a^\dagger(t)a^\dagger(t+\tau)a(t+\tau)a(t) \rangle / \langle a^\dagger a \rangle^2$, where a^\dagger and a are the single-mode creation and annihilation operators, respectively. For that purpose we have used the standard direct measurement approaching $g^{(2)}(\tau)$ for small mean number of photons [39]. At the same time, this detection scheme enables the estimation of photon number probability distribution with up to photon numbers limited by the overall measurement length, detection losses and photon generation rate. The detected photon clicks arrival times are recorded using a time tagging device with maximum resolution of 81 ps.

The results of the measurement of second-order correlation function for the laser frequency set on the resonance with the $5S_{1/2}(F=2) \leftrightarrow 5P_{1/2}(F'=2)$ transition and cavity transmission peak set to the energy difference between $5S_{1/2}(F=1) \leftrightarrow 5P_{1/2}(F'=2)$ levels are shown in Fig. 2. The excitation laser beam power has been set to 39.5 mW for which we have obtained the resulting average count rate on the three detectors $(437 \pm 7) \times 10^3$ counts/s. The spatial overlap of excitation and observation modes has been positioned approximately to the center of the atomic vapor cell with temperature of 61°C corresponding to the optical thickness of 0.78 ± 0.05 for the resonant $5S_{1/2}(F=2) \leftrightarrow 5P_{1/2}(F'=2)$ excitation. The displayed $g^2(\tau)$ corresponds to the average of the measurement on all three possible two-detector combinations with the overall measurement time of 130 minutes and the coincidence-detection window set to 324 ps. The evaluated peak value of $g^2(0) = 1.99 \pm 0.01$ from the data presented in the Fig. 2 suggests the generation of ideal thermal light field. Since we aim to evaluate the light source, the presented $g^2(\tau)$ has been corrected for the residual intrinsic detector dark counts of $(350 \pm 20, 180 \pm 13, 265 \pm 18)$ counts/s measured on the employed APD₁, APD₂ and APD₃, respectively. The raw value of $g^2(0)$ without correction on detector dark counts is 1.98 ± 0.01 . The red line in Fig. 2 corresponds to a theoretical fit using the normalized single-mode second-order correlation function for ideal thermal light $g^{(2)}(\tau) = 1 + |g^{(1)}(\tau)|^2$, where the first order correlation function $g^{(1)}(\tau)$ is modelled simply by assuming the Doppler broadened emission on the $5P_{1/2}(F'=2) \rightarrow 5S_{1/2}(F=1)$ transition followed by the spectral filtration by the Fabry-Pérot resonator with independently measured transmission bandwidth.

To further support our conclusions about the detection of the ideal thermal state, we measure the photocount statistics from which the photon number probability distribution $P(n)$ can be estimated. As the probability of the four-coincidence event detection for the observed thermal light count-rates and coincidence window

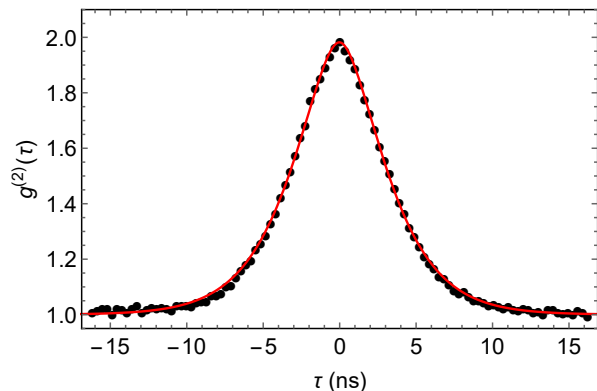


FIG. 2. The measured second-order correlation function $g^{(2)}(\tau)$. The measured data are represented by points, the solid red line corresponds to the theoretical fit by the simple theoretical model corresponding to the ideal single-mode thermal light. The size of the displayed data points corresponds to the single standard deviation error bars.

of 324 ps would be practically negligible even on the measurement time scales of days, it suffices to employ a three-detector scheme. The photon number probability distribution is estimated from the measured rates of singles, two-fold and three-fold coincidences using both the direct inversion [40] and the maximum-likelihood estimation [41]. The distributions resulting from the two methods differ only negligibly and within the largest error bar at $P(3)$ which has negligible effect on evaluated metrics, and we thus use and display only the distribution based on maximum likelihood algorithm, see Fig. 3. The estimated $P(n)$ corresponds to the ideal single-mode thermal light within statistical measurement errors, which certifies the unambiguous preparation of the ideal thermal light statistics. To illustrate the significance of the estimation of higher photon numbers in the presence of large attenuation, we show also the statistics of the ideal coherent state with the same mean photon number $\langle n \rangle = (1.47 \pm 0.01) \times 10^{-4}$ for comparison. The evaluated value of $g^2(0) = 1.99 \pm 0.01$ from full measured photon statistics corresponds to Mandel-Q parameter $Q = (1.46 \pm 0.01) \times 10^{-4}$, which is in good agreement with the theoretically expected value $Q_{\text{therm}} = 1.47 \times 10^{-4}$ for the ideal thermal state with given mean photon number. To characterize the quality of observed Bose-Einstein statistics, we employ the fundamental definition of the thermal light: it is light with maximum Shannon entropy $H = -\sum_n p(n) \log p(n)$ for the given mean number of photons. For the presented data $H = (144546 \pm 4) \times 10^{-8}$ in agreement with the theoretically expected $H_{\text{theory}} = 144546 \times 10^{-8}$. The actual distance between the ideal Bose-Einstein distribution and the measured one can be quantified by evaluation of the relative entropy $H(P(n)|P_{\text{ref}}(n))$, where $P_{\text{ref}}(n)$ corresponds to the reference probability distribution [42]. Advantageously, this distance is operational, it has a thermodynamical interpretation in terms of work

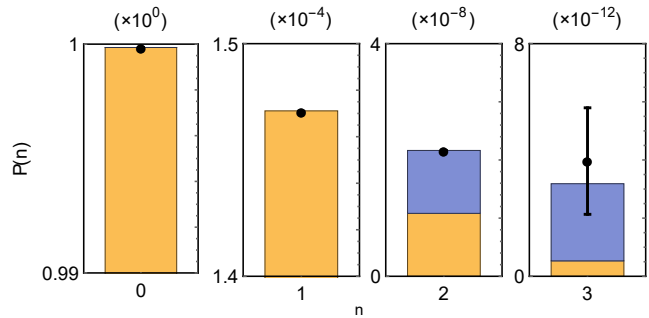


FIG. 3. The estimated photon number probability distribution (black points) with the blue and yellow bars corresponding to the theoretical photon number distributions for ideal thermal and coherent light fields with the same mean photon number, respectively, where the visible blue part shows the difference between these statistics. Error bars correspond to estimated single standard deviations, which are for the first three bars ($n=0,1,2$) smaller than the data point.

necessary to be done to reach the ideal thermal state from the measured one [43]. The evaluated relative Shannon entropies for the measured statistics with respect to ideal thermal and coherent state with the same mean photon numbers are $H(P(n)|P_{\text{therm}}(n)) = (8 \pm 7) \times 10^{-13}$ and $H(P(n)|P_{\text{coh}}(n)) = (413 \pm 5) \times 10^{-11}$, respectively. They further certify the relative thermodynamical closeness of the generated state to the ideal thermal state compared to a coherent state with the same energy. The uncertainties of the evaluated entropies have been estimated using the Monte Carlo routine from the uncertainties of the measured numbers of photon clicks.

III. LARGE-BANDWIDTH THERMAL LIGHT

The generation of thermal light using atomic vapors with high mean velocity thermal motional distribution corresponding to large Doppler broadening can naturally benefit from it and can be directly extended to frequency bandwidths at the order of several hundreds of MHz. We experimentally characterize such extension by measurement of the statistics of light emitted from warm Rb vapor by tuning several crucial parameters which directly influence the spectral and temporal width of the observed fluorescence. To allow the observation of narrow temporal wave packets, we replace the optical frequency filter in our setup by the Fabry-Pérot cavity with the free spectral range of about $\text{FSR} = 30$ GHz and measured transmission linewidth of $\Delta\nu = 818 \pm 3$ MHz (FWHM). The chosen $\Delta\nu$ is narrow compared to the hyperfine splitting of the excited $5P_{1/2}$ manifold and, at the same time, it allows for capturing of almost whole spectral width of Doppler-broadened emission for the considered Doppler broadening of about $\sigma_D = 260$ MHz. On the other hand, the large bandwidth of emitted photons will technically

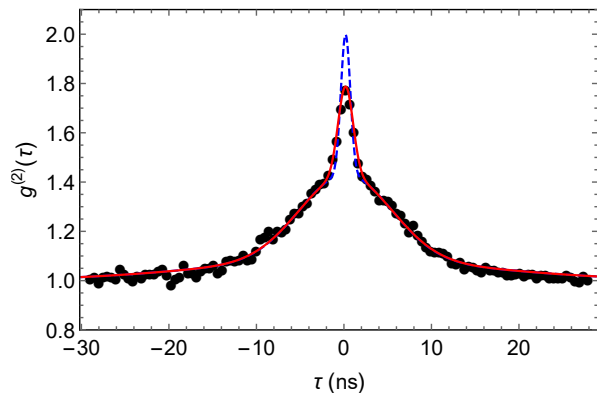


FIG. 4. The measured $g^{(2)}(\tau)$ with the broadband optical filtering fitted by the coherent superposition of Gaussian functions corresponding to single and multi-photon scattering (red solid line), see text for details. The blue dashed curve corresponds to the $g^{(2)}(\tau)$ obtained by the correction of the measured function on exactly measured timing uncertainties of employed single-photon detectors. The estimated error bars corresponds to the size of displayed data points.

compromise the direct observability of ideal thermal correlations due to the finite timing resolution of single-photon detectors. However, the precise knowledge of the exact time response of particular employed detectors allows recovering the true $g^{(2)}(0)$ values with high confidence.

Fig. 4 shows a typical measured second-order correlation function $g^{(2)}(\tau)$ with the broadband Fabry-Pérot optical filter. The excitation laser power has been set to $P = 39$ mW and the atomic cell temperature is corresponding to effective optical depth $OD = 1.19 \pm 0.08$. The observed temporal shape corresponds to two scattering processes, single-atom scattering and multi-atom scattering of detected photons, which give rise to two characteristic extents of reconstructed spectral widths [26, 44]. The presented data have been fitted using a simple theoretical model comprising two Gaussian spectra and the optical cavity filter with Lorentzian profile resulting in the estimated ratio of single to multi-photon scattering of 0.15. The maximal value of $g^{(2)}(0) = 1.71 \pm 0.03$ still corresponds to the ideal thermal state if we consider the timing jitter of employed detectors, whose effect can be unambiguously accounted for using the deconvolution of the measured $g^{(2)}(\tau)$ with their exact response function. The timing jitters have been precisely characterized in an independent measurement using fast mode-locked pulsed laser with pulse lengths of about 200 fs attenuated to single photon level and precise recording of the photon detection time. The evaluated timing uncertainties of $\sigma_1 = 358$ ps, $\sigma_2 = 551$ ps, $\sigma_3 = 365$ ps for APD₁ to APD₃, respectively, result in the corrected $g^{(2)}(0) = 2.00 \pm 0.04$, a clear signature of preserving the photon statistics of ideal thermal light. The frequency bandwidth of the detected light field has been estimated from the observed time spread in $g^{(2)}(\tau)$, which gives $\sigma_\tau = 13 \pm 2$ ns corre-

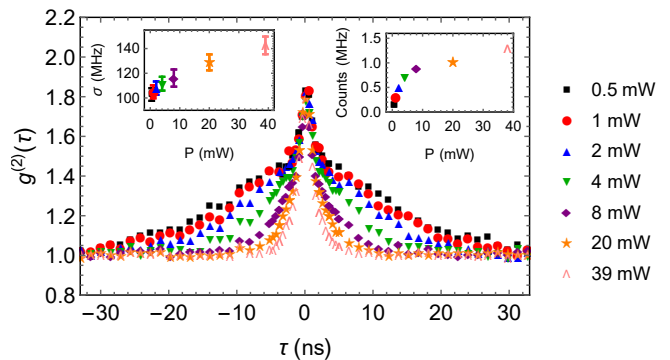


FIG. 5. The evaluated $g^{(2)}(\tau)$ functions measured for various powers of excitation laser beam. The two insets show the measured average count rates (right) and estimated thermal light frequency bandwidths (left). The estimated error bars correspond to a single standard deviation and are, where not directly illustrated, roughly the same size as plot markers.

sponding to $\sigma_\nu = 110 \pm 20$ MHz.

As can be seen in the Fig. 4, the overall temporal length of the generated thermal light is substantially broadened by the contribution of the single-atom or few-atom scattering processes. As demonstrated by A. Dussaux et al. [26], the contribution of the single atom scattering process to the observed $g^{(2)}(\tau)$ can be suppressed by maximization of the effective optical thickness, which can be achieved by resonant excitation and high atomic density. We have confirmed these observations and rest of presented results are thus realized for optical thickness of 1.19 ± 0.08 corresponding to maximal easily achievable temperature 70°C in our setup and resonant excitation on the $5S_{1/2}(F = 2) \leftrightarrow 5P_{1/2}(F' = 2)$ transition. The measured power dependence of the observed $g^{(2)}(\tau)$ correlations shown in the Fig. 5 suggests the convenience of increasing power for both the absolute observable spectral bandwidth and the detected photon count rate with the maximum values of $\sigma_\nu = 142 \pm 7$ MHz and 1.29×10^6 counts/s, respectively, corresponding to the maximal excitation laser power of 39 mW. We note that for all probed input laser powers, the observed values of $g^{(2)}(0)$ after correction for detector timing jitters lead to ideal thermal state value with accuracy within estimated errors one standard deviation.

In a quest for maximization of the generated thermal light bandwidth, we have examined the possibility of further suppression of the single-atom scattering contribution by measuring the $g^{(2)}(\tau)$ as a function of the spatial distance d defined as a distance between the cell output optical window and the observation region given by the intersection of excitation and observation spatial modes, see Fig. 1 for the spatial configuration. We choose d to be positive for the observation regions inside the atomic cell. The suppression of the single-atom scattering contribution is expected due to effective decreased number of atoms in the path of the photons scattered towards the analysis setup when shifting

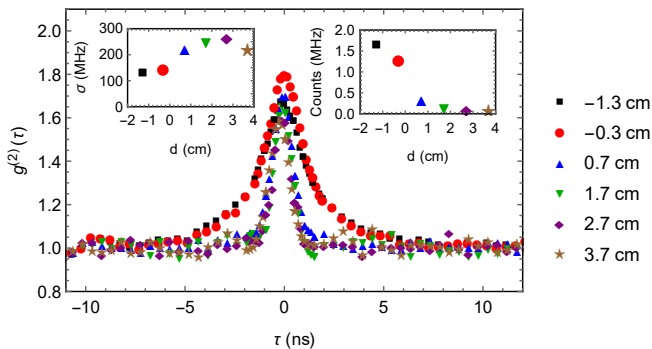


FIG. 6. The measured $g^{(2)}(\tau)$ of scattered light for various distances d of the rubidium cell output window from the center of the observation region defined by the intersection of the excitation and observation beam modes, see text and Fig. 1 for more details. The insets show the corresponding estimated light field spectral width (left) and detected count rate (right). The statistically estimated error bars correspond to one standard deviation, where indicated, otherwise they are below the extent of displayed data points.

the excitation-observation region towards the cell output window. The observed dependence presented in Fig. 6 for 39 mW excitation laser power suggests that positioning the interaction region to $d \geq 0.7$ cm inside the atomic cell almost fully suppresses the observed single scattering contribution and leads to thermal light spectral bandwidths of up to $\sigma_\nu = 270 \pm 20$ MHz. However, the increased length of the atomic medium which has to be passed by the resonant scattered light on its way to detection setup strongly suppresses the overall generated photon rate resulting in 3.4×10^5 counts/s corresponding to $\langle n \rangle = (1.6 \pm 0.1) \times 10^{-4}$. The scaling of the detected photon rate and spectral bandwidth can be seen in insets of the Fig. 6. The considered detected photon rate here corresponds to the sum of rates from all three detectors. The observable steep dependence of both the overall detected count rate and contribution of the single-atom scattering around $d \approx 0$ corresponds well to the spatial position of the interaction region at the cell window. To the best of our knowledge, the presented estimated spectral widths of the thermal light fields are by at least two

orders of magnitude better than any previously reported values achieved with pseudo thermal light sources [23] and, at the same time, the measured $g^{(2)}(0)$ values corrected for the detector timing jitter suggest the generation of the ideal single-mode thermal light.

IV. CONCLUSION AND OUTLOOK

We have demonstrated the generation of ideal thermal statistics of light field emitted from a warm atomic vapor. The evaluated $g^{(2)}(0) = 1.99 \pm 0.01$ together with the Bose-Einstein statistical distribution of the photon number probability without any correction on the finite detector time response represents, albeit theoretically expectable, long awaited and experimentally desired goal since pioneering experiments on detecting the statistical correlations of light emitted from low-pressure glow discharge lamps [45, 46]. We conclusively confirmed that Shannon entropy of the measured probability distribution corresponds to theoretically predicted one for the measured mean number of photons. Besides its fundamental interest, we have demonstrated that the thermal light generated from warm atomic vapor can benefit from the large Doppler-broadened spectral width of emitted photons, which is directly proportional to the atomic temperature. In addition, the presented thermal light bandwidth scalability to up to $\sigma_\nu = 270$ MHz goes in hand with the extreme technological simplicity of the scheme based on the bare single-pass excitation of warm atomic vapor. Together with observed high detected thermal photon rates of 3.4×10^5 counts/s, the presented source promises a substantial enhancement and speed up of a large number of applications in classical and quantum optics [8–16].

ACKNOWLEDGMENTS

This research has been supported by grant No. GA14-36681G of the Czech Science Foundation and Palacký University IGA-PrF-2017-008.

-
- [1] R. Hanbury Brown and R. Q. Twiss, *Nature* **177**, 27–29 (1956).
 - [2] R. Hanbury Brown and R. Q. Twiss, *Nature* **178**, 1046–1048 (1956).
 - [3] M. D. Eisaman, J. Fan, A. Migdall, and S. V. Polyakov, *Rev. Sci. Instr.* **82**, 071101 (2011).
 - [4] P. Lodahl, S. Mahmoodian, and S. Stobbe, *Rev. Mod. Phys.* **87**, 347 (2015), arXiv:1312.1079.
 - [5] L. Mandel, E. Wolf, *Optical Coherence and Quantum Optics* (Cambridge University Press, 1995).
 - [6] G. Breitenbach, S. Schiller, and J. Mlynek, *Nature* **387**, 471–475 (1997).
 - [7] A. I. Lvovsky, H. Hansen, T. Aichele, O. Benson, J. Mlynek, and S. Schiller, *Phys. Rev. Lett.* **87**, 050402 (2001), arXiv:quant-ph/0101051.
 - [8] G. Zambra, A. Andreoni, M. Bondani, M. Gramegna, M. Genovese, G. Brida, A. Rossi, and M. G. A. Paris, *Phys. Rev. Lett.* **95**, 063602 (2005), arXiv:quant-ph/0502060.
 - [9] G. Harder, D. Mogilevtsev, N. Korolkova, and Ch. Silberhorn, *Phys. Rev. Lett.* **113**, 070403 (2014), arXiv:1409.8076.
 - [10] L. Dvrat, M. Bakstein, D. Istrati, A. Shaham, and H. S. Eisenberg, *Opt. Express* **20**, 2266–2276 (2012), arXiv:1112.0914.

- [11] Y. Qu and S. Singh, *Opt. Commun.* **90**, 111-114 (1992).
- [12] A. Jechow, M. Seefeldt, H. Kurzke, A. Heuer, and R. Menzel, *Nat. Phot.* **7**, 973-976 (2013), arXiv:1310.4297.
- [13] K. Y. Spasibko, D. A. Kopylov, V. L. Krutyanskiy, T. V. Murzina, G. Leuchs, and M. V. Chekhova, *Phys. Rev. Lett.* **119**, 223603 (2017), arXiv:1705.07159.
- [14] D. Zhang, Y. H. Zhai and L. A. Wu, *Opt. Lett.* **30**, 2354-2356 (2005), arXiv:quant-ph/0503122.
- [15] A. Valencia, G. Scarcelli, M. D'Angelo, and Y. Shih, *Phys. Rev. Lett.* **94**, 063601 (2005), arXiv:quant-ph/0408001.
- [16] J. Sprigg, T. Peng, and Y. Shih, *Sci. Rep.* **6**, 38077 (2016), arXiv:1409.2134.
- [17] A. Zavatta, V. Parigi, and M. Bellini, *Phys. Rev. A* **75**, 052106 (2007), arXiv:0704.0179.
- [18] J. Roßnagel, S. T. Dawkins, K. N. Tolazzi, O. Abah, E. Lutz, F. Schmidt-Kaler, K. Singer, *Science* **352**, 325-329 (2016), arXiv:1510.03681.
- [19] C. Weedbrook, S. Pirandola, and T. C. Ralph, *Phys. Rev. A* **86**, 022318 (2012), arXiv:1110.4617.
- [20] F. T. Arecchi, *Phys. Rev. Lett.* **15**, 912 (1956).
- [21] M. Rousseau, *J. Opt. Soc. Am.* **61**, 1307-1316 (1971).
- [22] L. E. Estes, L. M. Narducci, and R. A. Tuft, *J. Opt. Soc. Am.* **61**, 1301-1306 (1971).
- [23] T. A. Kuusela, *American Journal of Physics* **85**, 289 (2017).
- [24] T. Gonsiorowski and J. C. Dainty, *J. Opt. Soc. Am.* **73**, 234-237 (1983).
- [25] K. Nakayama, Y. Yoshikawa, H. Matsumoto, Y. Torii and T. Kuga, *Opt. Express* **18**, 6604-6612 (2010).
- [26] A. Dussaux, T. Passerat de Silans, W. Guerin, O. Alibert, S. Tanzilli, F. Vakili, and R. Kaiser, *Phys. Rev. A* **93**, 043826 (2016), arXiv:1601.00853.
- [27] B. Blauensteiner, I. Herbauts, S. Betteli, A. Poppe and H. Hübel, *Phys. Rev. A* **79**, 063846 (2009), arXiv:0810.4785.
- [28] C. Shu, P. Chen, T. K. A. Chow, L. Zhu, Y. Xiao, M. M. T. Loy, and S. Du, *Nat. Commun.* **7**, 12783 (2016), arXiv:1602.08561.
- [29] X. Guo, C. Zou, C. Schuck, H. Jung, R. Cheng, and H. X Tang, *Light: Science and Applications* **6**, e16249 (2017), arXiv:1603.03726.
- [30] F. Boitier, A. Godar, E. Rosencher, and C. Fabre, *Nat. Phys.* **5**, 267-270 (2009).
- [31] H. Kurzke, J. Kiethe, A. Heuer and A. Jechow, *Laser Physics Letters* **14**, 055402 (2017), arXiv:1704.01096.
- [32] M. Blazek and W. Elsässer, *Phys. Rev. A* **84**, 063840 (2011).
- [33] P. K. Tan, G. H. Yeo, H. S. Poh, A. H. Chan, and C. Kurtsiefer, *Astrophys. J.* **789**, L10 (2014), arXiv:1403.7432.
- [34] X.-F. Liu, X.-H. Chen, X.-R. Yao, W.-K. Yu, G.-J. Zhai, and L.-A. Wu, *Opt. Lett.* **39**, 2314-2317 (2014).
- [35] S. Friberg, C. K. Hong, and L. Mandel, *Phys. Rev. Lett.* **54**, 2011-2013 (1985).
- [36] I. Abram, R. K. Raj, J. L. Oudar, and G. Dolique, *Phys. Rev. Lett.* **57**, 2516-2519 (1986).
- [37] B. Yurke and M. Potasek, *Phys. Rev. A* **36**, 3464 (1987).
- [38] C. F. McCormick, V. Boyer, E. Arimondo, and P. D. Lett, *Opt. Lett.* **32**, 178-180 (2007), arXiv:physics/0607254.
- [39] P. Grangier, G. Roger, and A. Aspect, *Europhys. Lett.* **1** 173-179 (1986).
- [40] J. Sperling, W. Vogel, and G. S. Agarwal, *Phys. Rev. A* **85**, 023820 (2012), arXiv:1202.5106.
- [41] Z. Hradil, J. Řeháček, J. Fiurášek, M. Ježek, in *Quantum State Estimation*, M. Paris, J. Řeháček, ed. (Springer, 2004).
- [42] S. Kullback and R. A. Leibler, *Annals of Mathematical Statistics* **22**, 79-86 (1951).
- [43] M. Esposito and C. Van den Broeck, *Europhysics Letters* **95**, 40004 (2011), arXiv:1104.5165.
- [44] J. C. de A. Carvalho, M. Oriá, M. Chevrollier, H. L. D. de S. Cavalcante and T. P. de Silans, *Phys. Rev. A* **91**, 053846 (2015), arXiv:1506.05683.
- [45] W. Martienssen and E. Spiller, *Am. J. of Phys.* **32**, 919 (1964).
- [46] B. L. Morgan and L. Mandel, *Phys. Rev. Lett.* **16**, 1012 (1966).